

REZERO: BOOSTING MCTS-BASED ALGORITHMS BY BACKWARD-VIEW AND ENTIRE-BUFFER REANALYZE

Anonymous authors

Paper under double-blind review

ABSTRACT

Monte Carlo Tree Search (MCTS)-based algorithms, such as MuZero and its derivatives, have achieved widespread success in various decision-making domains. These algorithms employ the *reanalyze* process to enhance sample efficiency from stale data, albeit at the expense of significant wall-clock time consumption. To address this issue, we propose a general approach named ReZero to boost tree search operations for MCTS-based algorithms. Specifically, drawing inspiration from the one-armed bandit model, we reanalyze training samples through a backward-view reuse technique which uses the value estimation of a certain child node to save the corresponding sub-tree search time. To further adapt to this design, we periodically reanalyze the entire buffer instead of frequently reanalyzing the mini-batch. The synergy of these two designs can significantly reduce the search cost and meanwhile guarantee or even improve performance, simplifying both data collecting and reanalyzing. Experiments conducted on Atari environments, DMControl suites and board games demonstrate that ReZero substantially improves training speed while maintaining high sample efficiency.

1 INTRODUCTION

As a pivotal subset of artificial intelligence, Reinforcement Learning (RL) (Sutton & Barto, 1988) has acquired achievements and applications across diverse fields, including interactive gaming (Vinyals et al., 2019), autonomous vehicles (Li et al., 2022), and natural language processing (Rafailov et al., 2023). Despite its successes, a fundamental challenge plaguing traditional model-free RL algorithms is their low sample efficiency. These algorithms typically require a large amount of data to learn effectively, making them often infeasible in the real-world scenarios. In response to this problem, numerous model-based RL methods (Janner et al., 2019; Hafner et al., 2020) have emerged. These methods involve learning an additional model of the environment from data and utilizing the model to assist the agent’s learning, thereby improving sample efficiency significantly.

Within this field, Monte Carlo Tree Search (MCTS) (Świechowski et al., 2023) has been proven to be a efficient method for utilizing models for planning. It incorporates the UCB1 algorithm (Auer et al., 2002) into the tree search process and has achieved promising results in a wide range of scenarios. Specifically, AlphaZero (Silver et al., 2017) plays a big role in combining deep reinforcement learning with MCTS, achieving notable accomplishments that can beat top-level human players. While it can only be applied to environments with perfect simulators, MuZero (Schrittwieser et al., 2019) extended the algorithm to cases without known environment models, resulting in good performances in a wider range of tasks. Following MuZero, many successor algorithms have emerged, enabling MuZero to be applied in continuous action spaces (Hubert et al., 2021), offline RL training scenarios (Schrittwieser et al., 2021), and etc. All these MCTS-based algorithms made valuable contributions to the universal applicability of the MCTS+RL paradigm.

However, the extensive tree search computations incur additional time overhead for these algorithms: During the data collection phase, the agent needs to execute MCTS to select an action every time it receives a new state. Furthermore, due to the characteristics of tree search, it is challenging to parallelize it using commonly used vectorized environments (Weng et al., 2022), further amplifying the speed disadvantage. On the other hand, during the reanalyze (Schrittwieser et al., 2021) process, in order to obtain higher-quality update targets, the latest models are used to re-run MCTS on the training mini-batch. The wall-clock time thus increases as a trade-off for high sample efficiency. The excessive cost has become a bottleneck hindering the further promotion of these algorithms.

054 Recently, a segment of research endeavors are directed toward mitigating the above wall-clock time
 055 overhead. On the one hand, SpeedyZero (Mei et al., 2023) diminishes algorithms’ time overheads
 056 by deploying a parallel execution training pipeline; however, it demands additional computational
 057 resources. On the other hand, it remains imperative to identify methodologies that accelerate these
 058 algorithms without imposing extra demands. PTSAZero (Fu et al., 2023), for instance, compresses
 059 the search space via state abstraction, decreasing the time cost per search. In contrast, we aim to
 060 adopt a method that is orthogonal to both of the previous approaches. It does not require state space
 061 compression but directly reduces the search space through value estimation, and it does not introduce
 062 additional hardware overhead.

063 In this paper, we introduce ReZero, a new approach/framework designed to boost the MCTS-based
 064 algorithms. Firstly, inspired by the one-armed bandit model (Lattimore & Szepesvári, 2020), we
 065 propose a backward-view reanalyze technique that proceeds in the reverse direction of the trajec-
 066 tories, utilizing previously searched root values to bypass the exploration of specific child nodes,
 067 thereby saving time. Additionally, we have proven the convergence of our search mechanism based
 068 on the non-stationary bandit model, i.e., the distribution of child node visits will concentrate on the
 069 optimal node. Secondly, to better adapt to our proposed backward-view reanalyze technique, we
 070 have devised a novel pipeline that concentrates MCTS calls within the reanalyze process and peri-
 071 odically reanalyzes the entire buffer after a fixed number of training iterations. This entire-buffer
 072 reanalyze not only reduces the number of MCTS calls but also better leverages the speed advantages
 073 of parallelization. Skipping the search of specific child nodes can be seen as a pruning operation,
 074 which is common in different tree search settings. Reanalyze is also a common module in MCTS-
 075 based algorithms. Therefore, our algorithm design is universal and can be easily applied to the
 076 MCTS-based algorithm family. In addition, it will not bring about any overhead in computation
 077 resources. Empirical experiments (Section 5) show that our approach yields good results in both
 078 single-agent discrete-action environment (Atari (Bellemare et al., 2013)), two-player board games
 079 (Silver et al., 2016), and continuous control suites (Tunyasuvunakool et al., 2020), greatly improv-
 080 ing the training speed while maintaining or even improving sample efficiency. Ablation experiments
 081 explore the impact of different reanalyze frequencies and the acceleration effect of backward-view
 082 reuse on a single search. The main contributions of this paper can be summarized as follows:

- 082 • We design a method to speed up a single tree search by the backward-view reanalyze technique.
 083 Theoretical support for the convergence of our proposed method is also provided.
- 084 • We propose an efficient framework with the entire-buffer reanalyze mechanism that further re-
 085 duces the number of MCTS calls and enhance its parallelization, thus boosting MCTS-based al-
 086 gorithms.
- 087 • We conduct experiments on diverse environments and investigate ReZero through ablations.

088 2 RELATED WORK

089 2.1 MCTS-BASED ALGORITHMS

092 AlphaGo (Silver et al., 2016) and AlphaZero (Silver et al., 2017) combined MCTS with deep RL,
 093 achieving significant results in board games, defeating world-champion players, and revealing their
 094 remarkable capabilities. Following these achievements, MuZero (Schrittwieser et al., 2019) com-
 095 bines tree search with a learned value equivalent model (Grimm et al., 2020b), successfully promot-
 096 ing the algorithm’s application to scenarios without known models, such as Atari. Subsequent to
 097 MuZero’s development, several new works based on the MuZero framework emerged. EfficientZero
 098 (Ye et al., 2021) further improved MuZero’s sample efficiency, using very little data for training and
 099 still achieving outstanding performance. Another works (Hubert et al., 2021; Antonoglou et al.,
 100 2021) extended the MuZero agent to environments with large action spaces and stochastic environ-
 101 ments, further broadening the algorithm’s usage scenario. MuZero Unplugged (Schrittwieser et al.,
 102 2021) applied MuZero’s reanalyze operation as a policy enhancement operator and extended it to
 103 offline settings. Despite the aforementioned excellent improvement techniques, the time overhead
 104 of MCTS-based RL remains significant, which is the main problem this paper aims to address.

105 2.2 MCTS ACCELERATION

106 Recent research has focused on accelerating MCTS-based algorithms. Mei et al. (2023) reduces the
 107 algorithm’s time overhead by designing a parallel system; however, this method requires more com-
 putational resources and involves some adjustments for large batch training. Fu et al. (2023) narrows

the search space through state abstraction, which amalgamates redundant information, thereby reducing the time cost per search. KataGo (Wu, 2019) use a naive information reuse trick. They save sub-trees of the search tree and serve as initialization for the next search. However, our proposed backward-view reanalyze technique is fundamentally different from this naive forward-view reuse and can enhance search results while saving time. To our knowledge, we are the first to enhance MCTS by reusing information in a backward-view. Our proposed approach can seamlessly integrate with various MCTS-based algorithms, many of which (Mei et al., 2023; Fu et al., 2023; Danihelka et al., 2022; Leurent & Maillard, 2020) are orthogonal to our contributions.

3 PRELIMINARIES

3.1 MUZERO

MuZero (Schrittwieser et al., 2019) is a fundamental model-based RL algorithm that incorporates a value-equivalent model (Grimm et al., 2020a) and leverages MCTS for planning within a learned latent space. The model consists of three core components: a *representation* model h_θ , a *dynamics* model g_θ , and a *prediction* model f_θ :

$$\begin{aligned} \text{Representation:} \quad & s_t = h_\theta(o_{t-l:t}) \\ \text{Dynamics:} \quad & s_{t+1}, r_t = g_\theta(s_t, a_t) \\ \text{Prediction:} \quad & v_t, p_t = f_\theta(s_t) \end{aligned} \tag{1}$$

The representation model transforms *last* observation sequences $o_{t-l:t}$ into a corresponding latent state s_t . The dynamics model processes this latent state alongside an action a_t , yielding the next latent state s_{t+1} and an estimated reward r_t . Finally, the prediction model accepts a latent state and produces both the predicted policy p_t and the state’s value v_t . These outputs are instrumental in guiding the agent’s action selection throughout its MCTS. Lastly the agent samples the best action a_t following the searched visit count distribution. MuZero *Reanalyze* is an advanced version of the original MuZero. This variant enhances the model’s accuracy by conducting a fresh MCTS on sampled states with the latest model, subsequently utilizing the refined policy from this search to update the policy targets. Such reanalysis yields targets of superior quality compared to those obtained during the initial data collection. Traditional uses of the algorithm have intertwined reanalysis with training, while we *suggest* a novel paradigm, advocating for the decoupling of the reanalysis process from training iterations, thus providing a more flexible and efficient methodology. Refer to the Appendix B for more details on MuZero during the training and inference phases.

3.2 BANDIT-VIEW TREE SEARCH

A stochastic bandit has K arms, and playing each arm means sampling a reward from the corresponding distribution. For a search tree in MCTS, the root node can be seen as a bandit, with each child node as an arm. The left side of Figure 1 illustrates this idea. However, as the policy is continuously improved during the search process, the reward distribution for the arms should change over time. Therefore, UCT (Kocsis & Szepesvári, 2006) modeled the root node as a non-stationary stochastic bandit with a drift condition:

$$\mathbb{P}(\hat{\mu}_{is} - \mu_i \geq \varepsilon) \leq \exp\left(-\frac{\varepsilon^2 s}{C^2}\right) \text{ and } \mathbb{P}(\hat{\mu}_{is} - \mu_i \leq -\varepsilon) \leq \exp\left(-\frac{\varepsilon^2 s}{C^2}\right) \tag{2}$$

Where $\hat{\mu}_{is}$ is the average reward of the first s samples of arm i . μ_i is the limit of $\mathbb{E}[\hat{\mu}_{is}]$ as s approaches infinity, which indicates that the expectation of the node value converges. C is an appropriate constant characterizes the rate of concentration.

Based on this modeling, UCT uses the bandit algorithm UCB1 (Auer et al., 2002) to select child nodes. AlphaZero inherits this concept and employs a variant formula:

$$UCB_{score}(s, a) = Q(s, a) + cP(s, a) \frac{\sqrt{\sum_b N(s, b)}}{1 + N(s, a)} \tag{3}$$

where s is the state corresponding to the current node, a is the action corresponding to a child node. $Q(s, a)$ is the mean return of choosing action a , $P(s, a)$ is the prior score of action a , $N(s, a)$ is the total time that a has been chosen, $\sum_b N(s, b)$ is the total time that s has been visited. Viewing tree search from the bandit-view inspired us to use techniques from the field of bandits to improve the tree search. In next section, We use the idea of the one-armed bandit model to design our algorithm and prove the convergence of our algorithm based on the non-stationary bandit model.

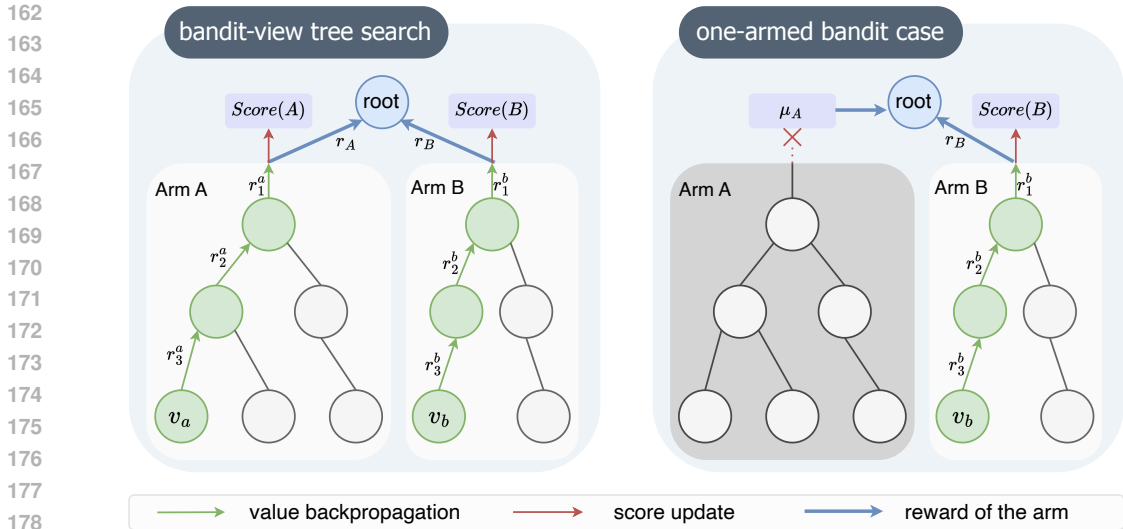


Figure 1: The connection between MCTS and bandits. **Left** shows tree search in a bandit-view. When the action A is selected, a **return** r_A will be returned, where $r_A = \sum_{t=1}^3 \gamma^{t-1} r_t^a + \gamma^3 v_a$. For the root node, the traversal, evaluation and back-propagation occurring in the sub-tree can be approximated as sampling from a non-stationary distribution. Thus it can be seen as a non-stationary bandit. **Right** shows the one-armed bandit case. Once the true value μ_A is known, we can evaluate arm A using μ_A , thereby eliminating the need to rely on subsequent tree search processes.

4 METHOD

In this section, we introduce the specific design of ReZero. Section 4.1 describes the inspiration and specific operations of backward-view reanalyze. It performs a reverse search on the trajectory and uses the value estimation of a certain child node to save the corresponding sub-tree search time. Section 4.2 analyzes the node selection method introduced in Section 4.1 and ultimately proves the convergence of the method. Section 4.3 introduced the overall framework of ReZero, which adopts the buffer reanalyze setting to better integrate with the method described in Section 4.1.

4.1 BACKWARD-VIEW REANALYZE

Our algorithm design stems from a simple inspiration: if we could know the true state-value (e.g., expected long-term return) of a child node in advance, we could save the search for it, thus conserving search time. As shown on the right side of Figure 1, we directly use the true expectation μ_A to evaluate the quality of Arm A, thereby eliminating the need for the back-propagated value to calculate the score in Eq. 3. This results in the process occurring within the gray box in Figure 1 being omitted. Indeed, this situation can be well modeled as an **one-armed bandit** (Lattimore & Szepesvári, 2020), which also facilitates our subsequent theoretical analysis.

Driven by the aforementioned motivation, we aspire to obtain the expected return of a child node in advance. However, the true value is always unknown. Consequently, we resort to using the root value obtained from MCTS as an approximate substitute. Specifically, for two adjacent time steps S_0^1 and S_0^0 in Figure 2, when searching for state S_0^1 , the root node corresponds to a child node of S_0^0 . Therefore, the root value obtained can be utilized to assist the search for S_0^0 . However, there is a temporal contradiction. S_0^1 is the successor state of S_0^0 , yet we need to complete the search for S_0^1 first. Fortunately, this is possible during the reanalyze process.

During reanalyze, since the trajectories were already collected in the replay buffer, we can perform tree search in a backward-view, which searches the trajectory in a reverse order. Figure 2 illustrates a batch containing $n + 1$ trajectories, each of length $k + 1$, and S_l^t is the t -th state in the l -th trajectory. We first conduct a search for all S^k s, followed by a search for all S^{k-1} s, and so on. After we search

¹The subscript denotes the trajectory, the superscript denotes the time step in the trajectory.

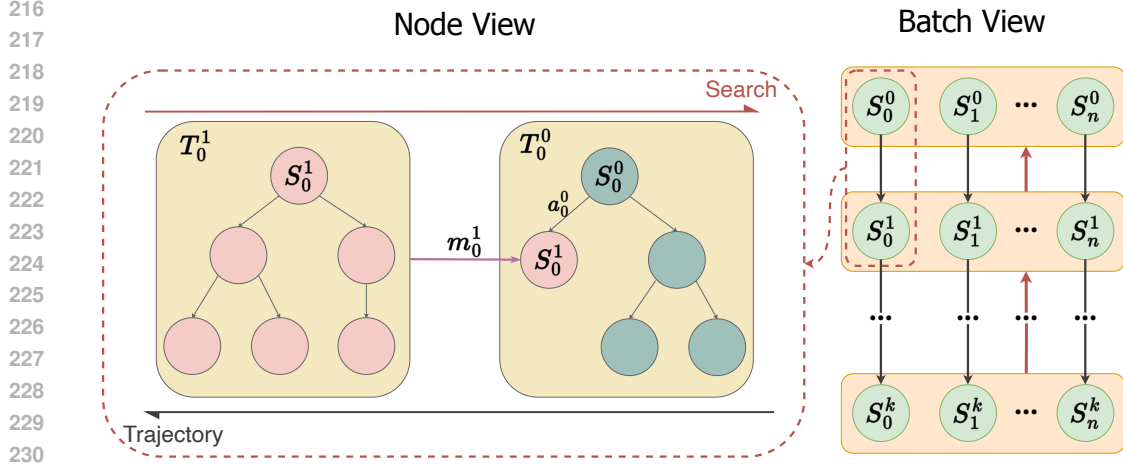


Figure 2: An illustration about the backward-view reanalyze in node and batch view. We sample $n + 1$ trajectories of length $k + 1$ to form a batch and conduct the search in the reverse direction of trajectories. From the node view, we would first search S_0^1 and then pass root value m_0^1 to S_0^0 to evaluate the value of a child node. T_0^1 and T_0^0 are the corresponding search trees. From the batch view, we would group all S^1 s into a sub batch to search together and pass the root values to the S^0 s.

on state S_l^{t+1} ², the root value m_l^{t+1} is obtained. When engaging in search on S_l^t , we assign the value of S_l^{t+1} to the fixed value m_l^{t+1} . During traverse in the tree, we select the action a_{root} for root node S_l^t with the following equation:

$$a_{root} = \arg \max_a I_l^t(a) \quad (4)$$

$$I_l^t(a) = \begin{cases} UCB_{score}(S_l^t, a), & a \neq a_l^t \\ r_l^t + \gamma m_l^{t+1}, & a = a_l^t \end{cases} \quad (5)$$

where a refers to the action associated with a child node, a_l^t is the action corresponding to S_l^{t+1} , and r_l^t signifies the reward predicted by the dynamic model. If an action distinct from a_l^t is selected, the simulation continues its traversal with the original setting as in MuZero. *If action a_l^t is selected, this simulation is terminated immediately.* Since the time used to search for node S_l^{t+1} is saved, this enhanced search process is faster than the original version. Algorithm 1 shows the specific design with Python-like code.³

Algorithm 1 Python-like code for information reuse

```

254 # trajectory_segment: a segment with length K      # N: simulation numbers during one search
255 def search_backwards(trajectory_segment):          def reuse_MCTS(root, action, values)
256     # prepare search context from the segment      for i in range(N):
257     roots, actions = prepare(trajectory_segment)  # select an action for root node
258     policy_targets = []                          a = select_root_child(root, action, value):
259     # search the roots backwards                  # early stop the simulation
260     for i in range(K, 1, -1):                    if a == action:
261         if i == K:                               backpropagate()
262             # origin MCTS for Kth root           break
263             policy, value = origin_MCTS(roots[i]) # traverse to the leaf node
264         else:                                     else:
265             # reuse information from previous sear # traverse()
266             policy, value = reuse_MCTS(          backpropagate()
267                 roots[i], actions[i], value
268             )
269     policy_targets.append(policy)

```

²To facilitate the explanation, we have omitted details such as the latent space and do not make a deliberate distinction between states and nodes.

³Our enhanced search process is implemented through `reuse_MCTS()`, where `select_root_child()` performs the action selection method of Equation 5. The `traverse()` and `backpropagate()` represent the forward search and backward propagation processes in standard MCTS.

4.2 THEORETICAL ANALYSIS

AlphaZero selects child nodes using Equation 3 and takes the final action based on the visit counts. In the previous section, we replace Equation 3 with Equation 5, which undoubtedly impacts the visit distribution of child nodes. Additionally, since we use the root value as an approximation to true expectation, the error between the two may also affect the search results. To demonstrate the reliability of our algorithm, in this section, we model the root node as a non-stationary bandit and prove that, as the number of total visit increases, the visit distribution gradually concentrates on the optimal arm. Specifically, we have the following theorem:

Theorem 1 For a non-stationary bandit that conforms to the assumptions of Equation 2, denote the total number of rounds as n , the prior score for arm i as P_i , and the number of times a sub-optimal arm i is selected in n rounds as $T_i(n)$, then use a sampled estimation instead of UCB value to evaluate a specific arm (like we do in Equation 5) can ensure that $\frac{\mathbb{E}[T_i(n)]}{n} \rightarrow 0$ as $n \rightarrow \infty$. Specifically, if we know the n times sample mean $\hat{\mu}^*$ of the optimal arm in advance, then $\mathbb{E}[T_i(n)]$ for all sub-optimal arm i satisfies

$$\mathbb{E}[T_i(n)] \leq 2 + \frac{2P_i\sqrt{n-1}}{\Delta_i - \varepsilon} + \frac{C^2}{(\Delta_i - \varepsilon)^2} + n \exp\left(-\frac{n\varepsilon^2}{C^2}\right) \quad (6)$$

Otherwise, if we have the n times sample mean $\hat{\mu}_l$ of a sub-optimal arm l , then for arm l ,

$$\mathbb{E}[T_l(n)] \leq 1 + \frac{2C^6}{\varepsilon^4 P_1^2} + n \exp\left(-\frac{n(\Delta_l - \varepsilon)^2}{C^2}\right) \quad (7)$$

and for other sub-optimal arms,

$$\mathbb{E}[T_i(n)] \leq 3 + \frac{2P_i\sqrt{n-1}}{\Delta_i - \varepsilon} + \frac{C^2}{(\Delta_i - \varepsilon)^2} + \frac{2C^6}{\varepsilon^4 P_1^2} \quad (8)$$

where Δ_i is the optimal gap for arm i , ε is a constant in $(0, \Delta_i)$, and C is the constant in Eq. 2.

We provide the complete proof and draw similar conclusions for AlphaZero in Appendix A. Additionally, our method has a lower upper bound for $\mathbb{E}[T_i(n)]$. This implies that our algorithm may yield visit distribution more concentrated on the optimal arm. This is a potential worth exploring in future work, especially in offline scenarios (Schrittwieser et al., 2021) where reanalyze becomes the sole method for policy improvement.

4.3 THE REZERO FRAMEWORK

The technique introduced in Section 4.1 will bring a new problem in practice. The experiments in the Appendix D.3 demonstrate that batching MCTS allows for parallel model inference and data processing, thereby accelerating the average search speed. However, as shown in the Figure 2, to conduct the backward-view reanalyze, we need to divide the batch into $\frac{1}{k+1}$ of its original size. This diminishes the benefits of parallelized search and, on the contrary, makes the algorithm slower.

We propose a new pipeline that is more compatible with the method introduced in Section 4.1. In particular, during the collect phase, we have transitioned from using MCTS to select actions to directly sampling actions based on the policy network’s output. This shift can be interpreted as an alternative method to augment exploration in the collect phase, akin to the noise injection at the root node in MCTS-based algorithms. Figure 11 in Appendix D.3 indicates that this modification does not significantly compromise performance during evaluation. For the reanalyze process, we introduce the periodical entire-buffer reanalyze. As shown in Figure 3, we reanalyze the whole buffer after a fixed number of training iterations. For each iteration, we do not need to run MCTS to reanalyze the mini-batch, only need to sample the mini-batch and execute the gradient descent.

Overall, this design offers two significant advantages: ① The entire buffer reanalyze is akin to the fixed target net mechanism in DQN (Mnih et al., 2013), maintaining a constant policy target for a certain number of training iterations. Reducing the frequency of policy target updates correspondingly decreases the number of MCTS calls. Concurrently, this does not result in a decrease in performance. ② Since we no longer invoke MCTS during the collect phase, all MCTS calls

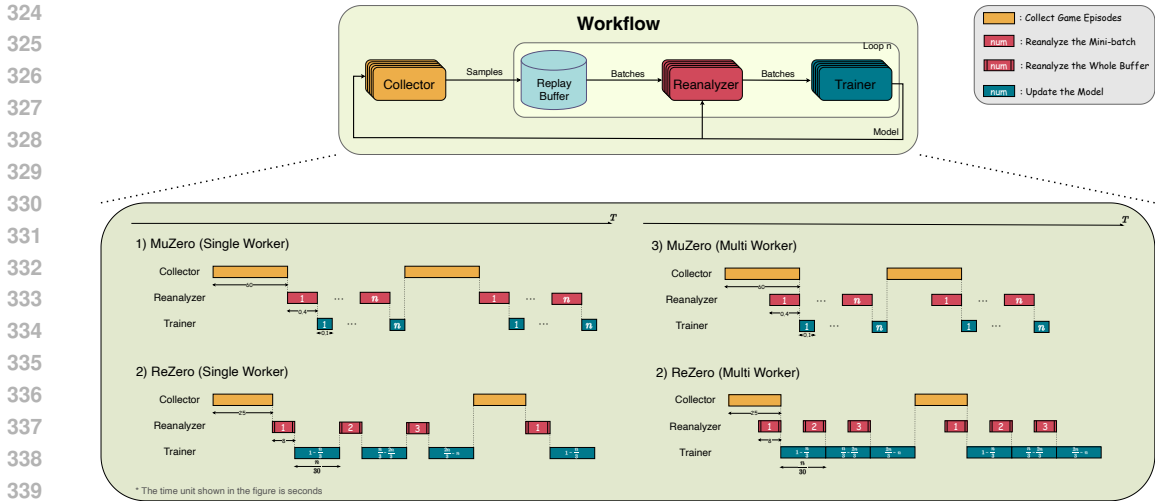


Figure 3: Execution workflow and runtime cycle graph about MuZero and ReZero in both single and multiple worker cases. The number inside the modules represent the number of iterations, and the number under the modules represent the time required for module execution. The model is updated n iterations between two collections. MuZero reanalyzes the mini-batch before each model update. ReZero reanalyzes the entire buffer after certain iterations ($\frac{n}{3}$ for example), which not only reduces the total number of MCTS calls, but also takes advantage of the processing speed of large batches.

are concentrated in the reanalyze process. And during the entire-buffer reanalyze, we are no longer constrained by the size of the mini-batch, allowing us to freely adjust the batch size to leverage the advantages of large batches. Figure 12 shows both excessively large and excessively small batch sizes can lead to a decrease in search speed. We choose the batch size of 2000 according to the experiment in Appendix D.3.

Experiments show that our algorithm maintains high sample efficiency and greatly save the running time of the algorithm. Our pipeline also has the following potential improvement directions:

- When directly using policy for data collection, action selection is no longer bound by tree search. Thus, previous vectorized environments like Weng et al. (2022) can be seamlessly integrated. Besides, this design makes MCTS-based algorithms compatible with existing RL exploration methods like Badia et al. (2020).
- Our method no longer needs to reanalyze the mini-batch for each iteration, thus decoupling the process of *reanalyze* and *training*. This provides greater scope for parallelization. In the case of multiple workers, we can design efficient parallelization paradigms as shown in Figure 3.
- We can use a more reasonable way, such as weighted sampling to preferentially reanalyze a part of the samples in the buffer, instead of simply reanalyzing all samples in the entire buffer. This is helpful to further reduce the computational overhead.

5 EXPERIMENT

Efficiency in RL usually refers to two aspects: *sample efficiency*, the agent’s ability to learn effectively from a limited number of environmental interactions, gauged by the samples needed to reach a successful policy using equal compute resources; *time efficiency*, which is how swiftly an algorithm learns to make optimal decisions, indicated by the wall-clock time taken to achieve a successful policy. **Our primary goal is to improve time efficiency without compromising sample efficiency.** Here we first give a toy example case in Section 5.1 to intuitively demonstrate the acceleration effect of our design, and the corresponding code example is placed in the Appendix D.4 for readers to quickly understand the algorithm design.

And then, to validate the efficiency of our introduced two boosting techniques for MCTS-based algorithms, we have incorporated the ReZero with two prominent algorithms detailed in Niu et al. (2023): MuZero with a Self-Supervised Learning loss (SSL) and EfficientZero, yielding the enhanced vari-

378
 379
 380
 381
 382
 383
 384
 385
 386
 387
 388
 389
 390
 391
 392
 393
 394
 395
 396
 397
 398
 399
 400
 401
 402
 403
 404
 405
 406
 407
 408
 409
 410
 411
 412
 413
 414
 415
 416
 417
 418
 419
 420
 421
 422
 423
 424
 425
 426
 427
 428
 429
 430
 431

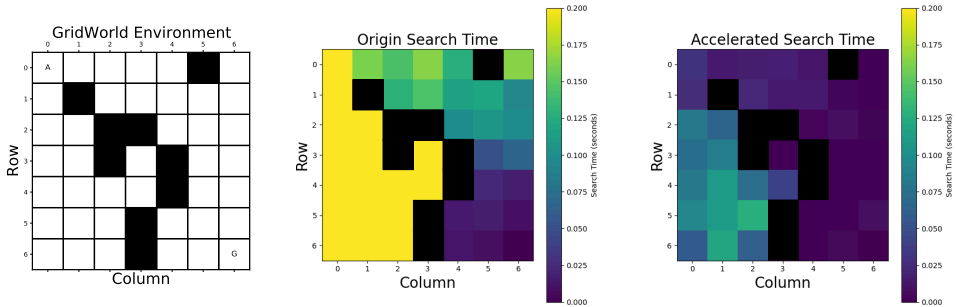


Figure 4: Acceleration effect on the toy case. **Left** is a simple maze environment where the agent starts at point A and receives a reward of size 1 upon reaching the end point G. **Middle** shows the search time corresponding to each position when set as the root node. Meanwhile, the root node values obtained during the search are preserved. **Right** shows the corresponding search time when these root node values are used to assist the search. The comparison shows that the search duration is generally reduced. For specific experimental settings and code, please refer to the Appendix D.4.

ants ReZero-M and ReZero-E respectively. For brevity, when the context is unambiguous, we simply refer to them as ReZero, omitting the symbol representing the baseline. It is important to highlight that ReZero can be seamlessly integrated with various algorithm variants of MuZero. In this context, we have chosen to exemplify this integration using the above two instances. In order to validate the applicability of our method across various decision-making environments, we opt for 26 representative Atari environments characterized by classic image-input observation and discrete action spaces, in addition to the strategic board games Connect4 and Gomoku with special state spaces, and two continuous control tasks in DMControl (Tunyasuvunakool et al., 2020). For a baseline comparison, we employed the original implementations of MuZero and EfficientZero as delineated in the LightZero benchmark (Niu et al., 2023). The full implementation details available in Appendix C. Besides, we emphasize that to ensure a fair comparison of wall-clock time, all experimental trials were executed on a fixed single worker hardware settings. In Section 5.2, Section 5.3 and Section 5.4, we sequentially explore and try to answer the following three questions:

- How much can ReZero-M/ReZero-E improve time efficiency compared to MuZero/EfficientZero, while maintaining equivalent levels of high sample efficiency?
- What is the effect and hyper-parameter sensitivity of the Entire-buffer Reanalyze technique?
- How much search budgets can be saved in practice by the Backward-view Reanalyze technique?

5.1 TOY CASE

Intuitively, it is evident that our proposed method can achieve a speed gain because we eliminate the search of a certain subtree, especially when this subtree corresponds to the optimal action (which often implies that the subtree has a larger number of nodes). We conduct an experiment on a toy example case and include the experimental code in the Appendix D.4. This helps to visually illustrate the speed gain achieved by skipping subtree search and allows readers to quickly understand the algorithm design through simple code. As shown in Figure 4 (Left), we implement a simple 7×7 maze environment where the agent starts at point A and receives a reward of 1 upon reaching point G. We perform an MCTS with each position in the maze as the root node and recorded the search time in Figure 4 (Middle). It can be seen that regions farther from the end point require more time to search (this is related to our simulation settings, see the appendix for details). For comparison, we also performed searches with each position as the root node, but during the search, we used the root node values obtained from the search in Figure 4 (Middle) to evaluate specific actions. The experimental time was recorded in Figure 4 (Right). It can be seen that after eliminating the search of specific subtrees, the search time was generally reduced. This simple result validates the rationality of our algorithm design. In the next section, we will specifically validate the time efficiency of the ReZero framework in diverse decision-making tasks in Section 5.2.

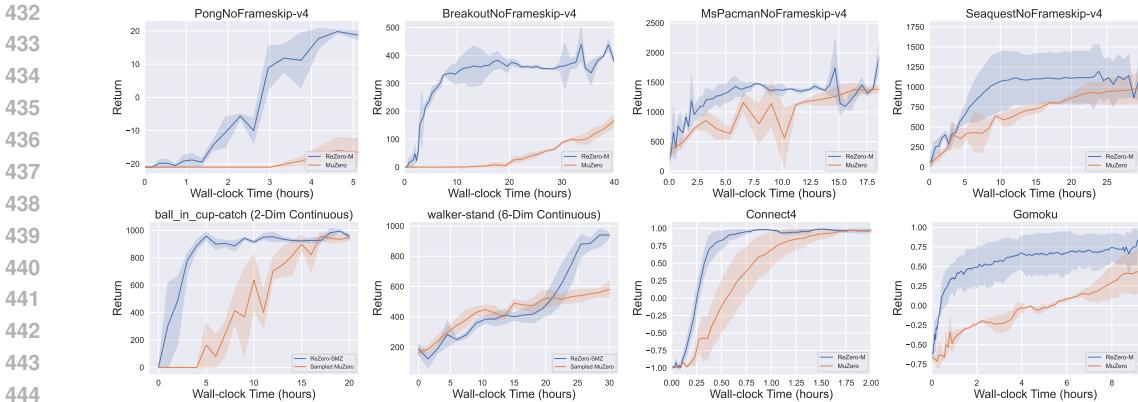


Figure 5: **Time-efficiency** of ReZero-M vs. MuZero on four representative *Atari* games, two continuous control tasks of *DMControl* (*ball_in_cup-catch*, *walker-stand*), and two board games (*Connect4*, *Gomoku*). The horizontal axis represents *Wall-clock Time* (hours), while the vertical axis indicates the *Episode Return* over 5 evaluation episodes. ReZero-M demonstrates superior time-efficiency compared to the baseline across a diverse set of games, encompassing both image and state observations, discrete and continuous actions, and scenarios involving sparse rewards. These figures compute mean of 5 runs, and shaded areas are 95% confidence intervals.

	Atari				DMControl		Board Games	
avg. wall time (h) to 100k env. steps ↓	Pong	Breakout	MsPacman	Seaquest	ball_in_cup-catch	walker-stand	Connet4	Gomoku
ReZero-M (ours)	1.0±0.1	3.0±0.8	1.4±0.2	1.9±0.4	2.1±0.2	4.3±0.3	5.5±0.6	4.5±0.5
MuZero (Schrittwieser et al., 2019)	4.0±0.5	4.9±1.8	6.9±0.3	10.1±0.5	5.6±0.4	9.5±0.6	9.1±0.8	15.3±1.5

Table 1: **Average wall-time** of ReZero-M vs. MuZero on various tasks. (*left*) Four *Atari* games, (*middle*) two control tasks, (*right*) two board games. The time represents the average total wall-time to 100k environment steps for each algorithm. Mean and standard deviation over 5 runs.

5.2 TIME EFFICIENCY

Setup: We aim to evaluate the performance of ReZero against classical MCTS-based algorithms MuZero and EfficientZero, focusing on the wall-clock time reduction required to achieve the comparable performance level. In order to facilitate a fair comparison in terms of wall-time, we not only utilize identical computational resources but also maintain consistent hyper-parameter settings across the algorithms (unless specified cases). Key parameters are aligned with those from original papers. After each data collection phase, the model is trained for multiple iterations according to the replay ratio, which is denoted as one training epoch. Specifically, we set the *replay ratio* (the ratio between environment steps and training steps) (D’Oro et al., 2022) to 0.25, and the *reanalyze ratio* (the ratio between targets computed from the environment and by reanalysing existing data) (Schrittwieser et al., 2021) is set to 1. For detailed hyper-parameter configurations, please refer to the Appendix C.

Results: Our experiments shown in Figure 5 illustrates the training curves and performance comparisons in terms of wall-clock time between ReZero-M and the MuZero across various decision-making environments. Note that on continuous control tasks we use the sampled version of ReZero-M and MuZero Hubert et al. (2021). The data clearly indicates that ReZero-M achieves a significant improvement in time efficiency, attaining a near-optimal policy in significantly less time for these eight diverse decision-making tasks. To provide an alternative perspective on the time cost of training on the same number of environment steps, we also provide an in-depth comparison of the wall-clock training time up to 100k environment steps for ReZero-M against MuZero in Table 1. For a more comprehensive understanding of our findings, we offer the complete table of the 26 *Atari* games usually used for sample-efficient RL in Appendix D.1. It reveals that, on most games, ReZero require between 2-4 times less wall-clock time per 100k steps compared to the baselines, while maintaining comparable or even superior performance in terms of episode return. Additional results about another algorithm comparison instance ReZero-E and EfficientZero are detailed in Appendix D.2, specifically in Figure 8 and 9. This setting also supports the time efficiency of our proposed ReZero framework.

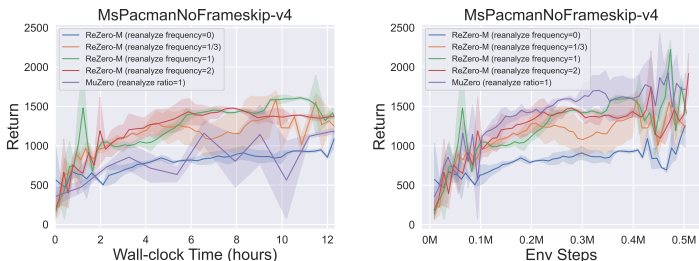


Figure 6: The ablation experiment of **Reanalyze Frequency** in ReZero-M on the Atari *MsPacman* game. The proper reanalyze frequency can improve time and sample efficiency while obtaining the comparable return with MuZero (*reanalyze ratio*=1).

5.3 EFFECT OF REANALYZE FREQUENCY

In next two sub-sections, we will delve into details to explain how ReZero works. Firstly, we will analyze how the entire-buffer reanalyze technique manages to simplify the original iterative mini-batch reanalyze scheme to the periodical updated version while maintaining high sample efficiency.

Here, we adjust the periodic *reanalyze frequency*—which determines how often the buffer is reanalyzed during a training epoch—in ReZero for the *MsPacman* environment. Specifically, we set *reanalyze frequency* to $\{0, \frac{1}{3}, 1, 2\}$. The original MuZero variants with the *reanalyze ratio* of 1 is also included in this ablation experiment as a baseline. Figure 6 shows entire training curves in terms of *Wall-time* or *Env Steps* and validates that appropriate reanalyze frequency can save the time overhead without causing any obvious performance loss.

5.4 EFFECT OF BACKWARD-VIEW REANALYZE

Indicators	Avg.time (ms)	tree search (num calls)	dynamics (num calls)	data process (num calls)
ReZero-M	0.69 ± 0.02	6089	122	277
MuZero	1.08 ± 0.09	13284	256	455

Table 2: Comparisons about the detailed time cost indicators between MuZero and ReZero-M inside the tree search.

To further validate and understand the advantages and significance of the backward-view reanalyze technique proposed in ReZero, we meticulously document a suite of statistical indicators of the tree search process in Table 2. The number of function calls is the cumulative value of 100 training iterations on *Pong*. *Avg. time* is the average time of a MCTS across all calls. Comparative analysis between ReZero-M and MuZero reveals that the backward-view reanalyze technique reduces the invocation frequency of the dynamics model, the search tree, and other operations like data process transformations. Consequently, this advanced technique in leveraging subsequent time step data contributes to save the tree search time in various MCTS-based algorithms, further leading to overall wall-clock time gains. The complexity and implementation of the tree search process directly influences the efficiency gains achieved through the backward-view reanalyze technique. As the tree search becomes more intricate and sophisticated, e.g. Sampled MuZero (Hubert et al., 2021), the time savings realized through this method are correspondingly amplified. Additionally, Theorem 1 demonstrates that the backward-view reanalyze can reduce the regret upper bound, which indicates a better search result. Besides, Figure 10 in Appendix D.3 shows a comparison of sample efficiency between using backward-view reanalyze and origin reanalyze process in *MsPacman*. The experimental results reveal that our method not only enhances the speed of individual searches but also improves sample efficiency. This aligns with the theoretical analysis.

6 CONCLUSION AND LIMITATION

In this paper, we have delved into the efficiency and scalability of MCTS-based algorithms. Unlike most existing works, we incorporate information reuse and periodic reanalyze techniques to reduce wall-clock time costs while preserving sample efficiency. Our theoretical analysis and experimental results confirm that ReZero efficiently reduces the time cost and maintains or even improves performance across different decision-making domains. However, our current experiments are mainly conducted on the single worker setting, there exists considerable optimization scope to apply our approach into distributed RL training, and our design harbors the potential of better parallel acceleration and more stable convergence in large-scale training tasks. Also, the combination between

ReZero and frameworks akin to AlphaZero, or its integration with some recent offline datasets such as RT-X (Padalkar et al., 2023), constitutes a fertile avenue for future research. These explorations could broaden the application horizons of MCTS-based algorithms. Additionally, since in offline training scenarios, reanalyze becomes the only means of policy improvement, this makes the acceleration of the reanalyze phase in ReZero even more critical. Moreover, the potential improvement in search results by ReZero may further improve the training result, rather than merely accelerating the training. Therefore, combining ReZero with MuZero Unplugged (Schrittwieser et al., 2021) is a direction worth exploring for building foundation models for decision-making.

REFERENCES

- Ioannis Antonoglou, Julian Schrittwieser, Sherjil Ozair, Thomas K Hubert, and David Silver. Planning in stochastic environments with a learned model. In *International Conference on Learning Representations*, 2021.
- Peter Auer, Nicolo Cesa-Bianchi, and Paul Fischer. Finite-time analysis of the multiarmed bandit problem. *Machine learning*, 47:235–256, 2002.
- Adrià Puigdomènech Badia, Pablo Sprechmann, Alex Vitvitskiy, Daniel Guo, Bilal Piot, Steven Kapturowski, Olivier Tieleman, Martín Arjovsky, Alexander Pritzel, Andrew Bolt, et al. Never give up: Learning directed exploration strategies. *arXiv preprint arXiv:2002.06038*, 2020.
- Marc G Bellemare, Yavar Naddaf, Joel Veness, and Michael Bowling. The arcade learning environment: An evaluation platform for general agents. *Journal of Artificial Intelligence Research*, 47: 253–279, 2013.
- Yuri Burda, Harrison Edwards, Amos Storkey, and Oleg Klimov. Exploration by random network distillation. *arXiv preprint arXiv:1810.12894*, 2018.
- Ivo Danihelka, Arthur Guez, Julian Schrittwieser, and David Silver. Policy improvement by planning with gumbel. In *International Conference on Learning Representations*, 2022.
- Pierluca D’Oro, Max Schwarzer, Evgenii Nikishin, Pierre-Luc Bacon, Marc G Bellemare, and Aaron Courville. Sample-efficient reinforcement learning by breaking the replay ratio barrier. In *Deep Reinforcement Learning Workshop NeurIPS 2022*, 2022.
- Yangqing Fu, Ming Sun, Buqing Nie, and Yue Gao. Accelerating monte carlo tree search with probability tree state abstraction. *arXiv preprint arXiv:2310.06513*, 2023.
- Christopher Grimm, André Barreto, Satinder Singh, and David Silver. The value equivalence principle for model-based reinforcement learning. *Advances in Neural Information Processing Systems*, 33:5541–5552, 2020a.
- Christopher Grimm, André Barreto, Satinder Singh, and David Silver. The value equivalence principle for model-based reinforcement learning. *Advances in Neural Information Processing Systems*, 33:5541–5552, 2020b.
- Danijar Hafner, Timothy Lillicrap, Mohammad Norouzi, and Jimmy Ba. Mastering atari with discrete world models. *arXiv preprint arXiv:2010.02193*, 2020.
- Matteo Hessel, Joseph Modayil, Hado Van Hasselt, Tom Schaul, Georg Ostrovski, Will Dabney, Dan Horgan, Bilal Piot, Mohammad Azar, and David Silver. Rainbow: Combining improvements in deep reinforcement learning. In *Proceedings of the AAAI conference on artificial intelligence*, volume 32, 2018.
- Thomas Hubert, Julian Schrittwieser, Ioannis Antonoglou, Mohammadamin Barekatin, Simon Schmitt, and David Silver. Learning and planning in complex action spaces. In Marina Meila and Tong Zhang (eds.), *Proceedings of the 38th International Conference on Machine Learning, ICML 2021, 18-24 July 2021, Virtual Event*, volume 139 of *Proceedings of Machine Learning Research*, pp. 4476–4486. PMLR, 2021. URL <http://proceedings.mlr.press/v139/hubert21a.html>.

- 594 Michael Janner, Justin Fu, Marvin Zhang, and Sergey Levine. When to trust your model: Model-
595 based policy optimization. *Advances in neural information processing systems*, 32, 2019.
596
- 597 Levente Kocsis and Csaba Szepesvári. Bandit based monte-carlo planning. In *European conference*
598 *on machine learning*, pp. 282–293. Springer, 2006.
- 599 Tor Lattimore and Csaba Szepesvári. *Bandit algorithms*. Cambridge University Press, 2020.
600
- 601 Edouard Leurent and Odalric-Ambrym Maillard. Monte-carlo graph search: the value of merging
602 similar states. In *Asian Conference on Machine Learning*, pp. 577–592. PMLR, 2020.
- 603 Quanyi Li, Zhenghao Peng, Lan Feng, Qihang Zhang, Zhenghai Xue, and Bolei Zhou. Metadrive:
604 Composing diverse driving scenarios for generalizable reinforcement learning. *IEEE Transactions*
605 *on Pattern Analysis and Machine Intelligence*, 2022.
606
- 607 Yixuan Mei, Jiakuan Gao, Weirui Ye, Shaohuai Liu, Yang Gao, and Yi Wu. Speedyzero: Mas-
608 tering atari with limited data and time. In *The Eleventh International Conference on Learning*
609 *Representations*, 2023.
- 610 Volodymyr Mnih, Koray Kavukcuoglu, David Silver, Alex Graves, Ioannis Antonoglou, Daan Wier-
611 stra, and Martin Riedmiller. Playing atari with deep reinforcement learning. *arXiv preprint*
612 *arXiv:1312.5602*, 2013.
613
- 614 Yazhe Niu, Yuan Pu, Zhenjie Yang, Xueyan Li, Tong Zhou, Jiyuan Ren, Shuai Hu, Hongsheng Li,
615 and Yu Liu. Lightzero: A unified benchmark for monte carlo tree search in general sequential
616 decision scenarios. *arXiv preprint arXiv:2310.08348*, 2023.
- 617 Abhishek Padalkar, Acorn Pooley, Ajinkya Jain, Alex Bewley, Alex Herzog, Alex Irpan, Alexander
618 Khazatsky, Anant Rai, Anikait Singh, Anthony Brohan, et al. Open x-embodiment: Robotic
619 learning datasets and rt-x models. *arXiv preprint arXiv:2310.08864*, 2023.
620
- 621 Tobias Pohlen, Bilal Piot, Todd Hester, Mohammad Gheshlaghi Azar, Dan Horgan, David Budden,
622 Gabriel Barth-Maron, Hado Van Hasselt, John Quan, Mel Večerík, et al. Observe and look further:
623 Achieving consistent performance on atari. *arXiv preprint arXiv:1805.11593*, 2018.
- 624 Rafael Rafailov, Archit Sharma, Eric Mitchell, Stefano Ermon, Christopher D Manning, and Chelsea
625 Finn. Direct preference optimization: Your language model is secretly a reward model. *arXiv*
626 *preprint arXiv:2305.18290*, 2023.
627
- 628 Tom Schaul, John Quan, Ioannis Antonoglou, and David Silver. Prioritized experience replay. *arXiv*
629 *preprint arXiv:1511.05952*, 2015.
- 630 Julian Schrittwieser, Ioannis Antonoglou, Thomas Hubert, Karen Simonyan, Laurent Sifre, Simon
631 Schmitt, Arthur Guez, Edward Lockhart, Demis Hassabis, Thore Graepel, Timothy P. Lillicrap,
632 and David Silver. Mastering atari, go, chess and shogi by planning with a learned model. *CoRR*,
633 abs/1911.08265, 2019. URL <http://arxiv.org/abs/1911.08265>.
- 634 Julian Schrittwieser, Thomas Hubert, Amol Mandhane, Mohammadamin Barekatin, Ioannis
635 Antonoglou, and David Silver. Online and offline reinforcement learning by planning with a
636 learned model. *Advances in Neural Information Processing Systems*, 34:27580–27591, 2021.
637
- 638 Max Schwarzer, Johan Samir Obando Ceron, Aaron Courville, Marc G Bellemare, Rishabh Agar-
639 wal, and Pablo Samuel Castro. Bigger, better, faster: Human-level atari with human-level effi-
640 ciency. In *International Conference on Machine Learning*, pp. 30365–30380. PMLR, 2023.
- 641 David Silver, Aja Huang, Chris J Maddison, Arthur Guez, Laurent Sifre, George Van Den Driessche,
642 Julian Schrittwieser, Ioannis Antonoglou, Veda Panneershelvam, Marc Lanctot, et al. Mastering
643 the game of go with deep neural networks and tree search. *nature*, 529(7587):484–489, 2016.
644
- 645 David Silver, Thomas Hubert, Julian Schrittwieser, Ioannis Antonoglou, Matthew Lai, Arthur Guez,
646 Marc Lanctot, Laurent Sifre, Dharshan Kumaran, Thore Graepel, et al. Mastering chess and shogi
647 by self-play with a general reinforcement learning algorithm. *arXiv preprint arXiv:1712.01815*,
2017.

- 648 R. S. Sutton and A. G. Barto. Reinforcement learning: An introduction. *IEEE Transactions on*
649 *Neural Networks*, 16:285–286, 1988.
- 650
- 651 Maciej Świechowski, Konrad Godlewski, Bartosz Sawicki, and Jacek Mańdziuk. Monte carlo tree
652 search: A review of recent modifications and applications. *Artificial Intelligence Review*, 56(3):
653 2497–2562, 2023.
- 654 Saran Tunyasuvunakool, Alistair Muldal, Yotam Doron, Siqi Liu, Steven Bohez, Josh Merel,
655 Tom Erez, Timothy Lillicrap, Nicolas Heess, and Yuval Tassa. dm control: Software and
656 tasks for continuous control. *Software Impacts*, 6:100022, 2020. ISSN 2665-9638. doi:
657 <https://doi.org/10.1016/j.simpa.2020.100022>. URL [https://www.sciencedirect.com/
658 science/article/pii/S2665963820300099](https://www.sciencedirect.com/science/article/pii/S2665963820300099).
- 659 Oriol Vinyals, Igor Babuschkin, Wojciech M. Czarnecki, Michaël Mathieu, Andrew Dudzik, Jun-
660 young Chung, David H. Choi, Richard Powell, Timo Ewalds, Petko Georgiev, Junhyuk Oh,
661 Dan Horgan, Manuel Kroiss, Ivo Danihelka, Aja Huang, Laurent Sifre, Trevor Cai, John P.
662 Agapiou, Max Jaderberg, Alexander Sasha Vezhnevets, Rémi Leblond, Tobias Pohlen, Valentin
663 Dalibard, David Budden, Yury Sulsky, James Molloy, Tom Le Paine, Çağlar Gülçehre, Ziyu
664 Wang, Tobias Pfaff, Yuhuai Wu, Roman Ring, Dani Yogatama, Dario Wünsch, Katrina McK-
665 inney, Oliver Smith, Tom Schaul, Timothy P. Lillicrap, Koray Kavukcuoglu, Demis Hassabis,
666 Chris Apps, and David Silver. Grandmaster level in starcraft II using multi-agent reinforce-
667 ment learning. *Nat.*, 575(7782):350–354, 2019. doi: 10.1038/s41586-019-1724-z. URL
668 <https://doi.org/10.1038/s41586-019-1724-z>.
- 669 Jiayi Weng, Min Lin, Shengyi Huang, Bo Liu, Denys Makoviichuk, Viktor Makoviychuk, Zichen
670 Liu, Yufan Song, Ting Luo, Yukun Jiang, et al. Envpool: A highly parallel reinforcement learning
671 environment execution engine. *Advances in Neural Information Processing Systems*, 35:22409–
672 22421, 2022.
- 673
- 674 David J Wu. Accelerating self-play learning in go. *arXiv preprint arXiv:1902.10565*, 2019.
- 675 Weirui Ye, Shaohuai Liu, Thanard Kurutach, Pieter Abbeel, and Yang Gao. Mastering atari games
676 with limited data. *Advances in Neural Information Processing Systems*, 34:25476–25488, 2021.
- 677
- 678
- 679
- 680
- 681
- 682
- 683
- 684
- 685
- 686
- 687
- 688
- 689
- 690
- 691
- 692
- 693
- 694
- 695
- 696
- 697
- 698
- 699
- 700
- 701

A PROOF MATERIALS

In this section, we will present the complete supplementary proofs.

Lemma A: Let w_t be a random variable that satisfies the concentration condition in Equation 2 with zero expectation, $\varepsilon > 0$, $a > 0$ and

$$\kappa = \sum_{t=1}^n \mathbb{I}\{w_t + \sqrt{\frac{a}{t^2}} \geq \varepsilon\} \quad (9)$$

then it holds that $E[\kappa] \leq 1 + \frac{2\sqrt{a}}{\varepsilon} + \frac{C^2}{\varepsilon^2}$.

Proof. Take u as $\frac{2\sqrt{a}}{\varepsilon}$, then

$$E[\kappa] \leq u + \sum_{t=\lceil u \rceil}^n \mathbb{P}(w_t + \sqrt{\frac{a}{t^2}} \geq \varepsilon) \quad (10)$$

$$\leq u + \sum_{t=\lceil u \rceil}^n \exp\left(-\frac{t(\varepsilon - \sqrt{\frac{a}{t^2}})^2}{C^2}\right) \quad (11)$$

$$\leq 1 + u + \int_u^\infty \exp\left(-\frac{t(\varepsilon - \sqrt{\frac{a}{t^2}})^2}{C^2}\right) dt \quad (12)$$

$$\leq 1 + u + e^{2\frac{\sqrt{a}\varepsilon}{C^2}} \int_u^\infty e^{-\frac{t\varepsilon^2}{C^2}} dt \quad (13)$$

$$= 1 + u + \frac{C^2}{\varepsilon^2} = 1 + \frac{2\sqrt{a}}{\varepsilon} + \frac{C^2}{\varepsilon^2} \quad (14)$$

□

Proof for Theorem 1:

Proof. We first present the upper bound of $\mathbb{E}[T_i(n)]$ for using the Equation 3 in AlphaZero. A slight adjustment to this proof yields the conclusion of Theorem 1. Denote $T_i(k)$ as the number of times that arm i has been chosen until time k , A_t as the arm selected at time t , $\hat{\mu}_{i_s}$ as the average of the first s samples of arm i , μ_i as the limit of $\mathbb{E}[\hat{\mu}_{i_s}]$, which satisfies the concentration assumption in Equation 2, and $\hat{\mu}_i(k) = \hat{\mu}_{iT_i(k)}$. Without loss of generality, we assume that arm 1 is the optimal arm. Then we have:

$$T_i(n) = \sum_{t=1}^n \mathbb{I}\{A_t = i\} \quad (15)$$

$$\leq \sum_{t=1}^n \mathbb{I}\{\hat{\mu}_1(t-1) + P_1 \frac{\sqrt{t-1}}{1+T_1(t-1)} \leq \mu_1 - \varepsilon\} \quad (16)$$

$$+ \sum_{t=1}^n \mathbb{I}\{\hat{\mu}_i(t-1) + P_i \frac{\sqrt{t-1}}{1+T_i(t-1)} \geq \mu_1 - \varepsilon \text{ and } A_t = i\} \quad (17)$$

for Equation 16, we have

$$\mathbb{E}\left[\sum_{t=1}^n \mathbb{I}\left\{\hat{\mu}_1(t-1) + P_1 \frac{\sqrt{t-1}}{1+T_1(t-1)} \leq \mu_1 - \varepsilon\right\}\right] \quad (18)$$

$$\leq 1 + \sum_{t=2}^n \sum_{s=0}^{t-1} \mathbb{P}\left(\hat{\mu}_{1s} + P_1 \frac{\sqrt{t-1}}{1+s} \leq \mu_1 - \varepsilon\right) \quad (19)$$

$$= 1 + \sum_{t=2}^n \sum_{s=1}^{t-1} \mathbb{P}\left(\hat{\mu}_{1s} + P_1 \frac{\sqrt{t-1}}{1+s} \leq \mu_1 - \varepsilon\right) \quad (20)$$

$$\leq 1 + \sum_{t=2}^n \sum_{s=1}^{t-1} \exp\left(-\frac{s(\varepsilon + P_1 \frac{\sqrt{t-1}}{1+s})^2}{C^2}\right) \quad (21)$$

$$\leq 1 + \sum_{t=2}^n \exp\left(-\frac{1}{C^2} \varepsilon P_1 \sqrt{t-1}\right) \sum_{s=1}^{t-1} \exp\left(-\frac{s\varepsilon^2}{C^2}\right) \quad (22)$$

$$\leq 1 + \sum_{t=2}^n \exp\left(-\frac{1}{C^2} \varepsilon P_1 \sqrt{t-1}\right) \frac{C^2}{\varepsilon^2} \quad (23)$$

$$\leq 1 + \frac{2C^6}{\varepsilon^4 P_1^2} \quad (24)$$

Notes: In Equation 19, since we assume $P_1 \geq \mu_1$, the probability of the term $s = 0$ would be 0. Thus, we can discard it. If this assumption doesn't hold, we can choose to accumulate t starting from a larger t_0 (which satisfies $P_1 \sqrt{t_0 - 1} > \mu_1$ as mentioned in the article). Starting the summation from such a t_0 ensures all terms of $s = 0$ can still be discarded, and all add terms that $t \leq t_0$ can be bounded to 1. This only changes the constant term and won't affect the growth rate of regret. From Equation 21 to Equation 22, we just need to expand the quadratic term and do some simple inequality scaling. From Equation 22 to Equation 23, we need to notice that $\sum_{s=1}^{t-1} \exp(-\frac{s\varepsilon^2}{C^2})$ is a geometric sequence and scale it to $\frac{C^2}{\varepsilon^2}$. From Equation 23 to Equation 24, we use the inequality $\sum_{t=2}^n \frac{1}{e^{a\sqrt{t-1}}} \leq \int_1^\infty \frac{1}{e^{a\sqrt{t-1}}}$.

And for Equation 17, we have

$$\mathbb{E}\left[\sum_{t=1}^n \mathbb{I}\left\{\hat{\mu}_i(t-1) + P_i \frac{\sqrt{t-1}}{1+T_i(t-1)} \geq \mu_1 - \varepsilon \text{ and } A_t = i\right\}\right] \quad (25)$$

$$\leq \mathbb{E}\left[\sum_{t=1}^n \mathbb{I}\left\{\hat{\mu}_i(t-1) + P_i \sqrt{\frac{n-1}{(1+T_i(t-1))^2}} \geq \mu_1 - \varepsilon \text{ and } A_t = i\right\}\right] \quad (26)$$

$$\leq 1 + \mathbb{E}\left[\sum_{s=1}^{n-1} \mathbb{I}\left\{\hat{\mu}_{is} + P_i \sqrt{\frac{n-1}{(1+s)^2}} \geq \mu_1 - \varepsilon\right\}\right] \quad (27)$$

$$\leq 1 + \mathbb{E}\left[\sum_{s=1}^n \mathbb{I}\left\{\hat{\mu}_{is} - \mu_i + P_i \sqrt{\frac{n-1}{s^2}} \geq \Delta_i - \varepsilon\right\}\right] \quad (28)$$

with Lemma A, we can have

$$28 \leq 2 + \frac{2P_i \sqrt{n-1}}{\Delta_i - \varepsilon} + \frac{C^2}{(\Delta_i - \varepsilon)^2} \quad (29)$$

so we have

$$\mathbb{E}[T_i(n)] \leq 3 + \frac{2P_i \sqrt{n-1}}{\Delta_i - \varepsilon} + \frac{C^2}{(\Delta_i - \varepsilon)^2} + \frac{2C^6}{\varepsilon^4 P_1^2} \quad (30)$$

The proof of theorem 1 can be obtained by making slight modifications. In case we have drawn n samples from the same non-stationary distribution as arm 1, and the average of these first n samples is $\hat{\mu}_1$,

$$\mathbb{E}[T_i(n)] = \mathbb{E}\left[\sum_{t=1}^n \mathbb{I}\{A_t = i\}\right] \quad (31)$$

$$\leq \mathbb{E}\left[\sum_{t=1}^n \mathbb{I}\{\hat{\mu}_1 \leq \mu_1 - \varepsilon\}\right] \quad (32)$$

$$+ \mathbb{E}\left[\sum_{t=1}^n \mathbb{I}\left\{\hat{\mu}_i(t-1) + P_i \frac{\sqrt{t-1}}{1+T_i(t-1)} \geq \mu_1 - \varepsilon \text{ and } A_t = i\right\}\right] \quad (33)$$

$$\leq n \exp\left(-\frac{n\varepsilon^2}{C^2}\right) + \mathbb{E}\left[\sum_{t=1}^n \mathbb{I}\left\{\hat{\mu}_i(t-1) + P_i \frac{\sqrt{t-1}}{1+T_i(t-1)} \geq \mu_1 - \varepsilon \text{ and } A_t = i\right\}\right] \quad (34)$$

$$\leq 2 + \frac{2P_i\sqrt{n-1}}{\Delta_i - \varepsilon} + \frac{C^2}{(\Delta_i - \varepsilon)^2} + n \exp\left(-\frac{n\varepsilon^2}{C^2}\right) \quad (35)$$

In case we have drawn n samples from the same non-stationary distribution as arm l , and the average of these first n samples is $\hat{\mu}_l$,

$$\mathbb{E}[T_l(n)] = \mathbb{E}\left[\sum_{t=1}^n \mathbb{I}\{A_t = l\}\right] \quad (36)$$

$$\leq \mathbb{E}\left[\sum_{t=1}^n \mathbb{I}\left\{\hat{\mu}_1(t-1) + P_1 \frac{\sqrt{t-1}}{1+T_1(t-1)} \leq \mu_1 - \varepsilon\right\}\right] \quad (37)$$

$$+ \mathbb{E}\left[\sum_{t=1}^n \mathbb{I}\{\hat{\mu}_l \geq \mu_1 - \varepsilon \text{ and } A_t = l\}\right] \quad (38)$$

$$\leq \mathbb{E}\left[\sum_{t=1}^n \mathbb{I}\left\{\hat{\mu}_1(t-1) + P_1 \frac{\sqrt{t-1}}{1+T_1(t-1)} \leq \mu_1 - \varepsilon\right\}\right] + n \exp\left(-\frac{n(\Delta_l - \varepsilon)^2}{C^2}\right) \quad (39)$$

$$\leq 1 + \frac{2C^6}{\varepsilon^4 P_1^2} + n \exp\left(-\frac{n(\Delta_l - \varepsilon)^2}{C^2}\right) \quad (40)$$

and the bound of $E[T_i(n)]$ for $i \neq l$ keeps unchanged. \square

B MUZERO

During the *inference* phase, the representation model transforms a sequence of the last l observations $o_{t-l:t}$ into a corresponding latent state representation s_t . The dynamics model processes this latent state alongside an action a_t , yielding the subsequent latent state s_{t+1} and an estimated reward r_t . Finally, the prediction model accepts a latent state and produces both the predicted policy p_t and the state's value estimate v_t . These outputs are instrumental in guiding the agent's action selection process throughout its MCTS. Lastly the agent selects or samples the best action a_t following the searched visit count distribution. During the *training* phase, given a training sequence $\{o_{t-l:t+K}, a_{t+1:t+K}, u_{t+1:t+K}, \pi_{t+1:t+K}, z_{t+1:t+K}\}$ at time t sampled from the replay buffer, where u_{t+k} denotes the actual reward obtained from the environment, π_{t+k} represents the target policy obtained through MCTS during the agent-environment interaction, and z_{t+k} is the value target computed using *n-step bootstrapping* [Hessel et al. \(2018\)](#). The representation model initially converts the sequence of observations $o_{t-l:t}$ into the latent state s_t^0 . Subsequently, the dynamic model executes K latent space rollouts based on the sequence of actions $a_{t+1:t+K}$. The latent state derived after the k -th rollout is denoted as s_t^k , with the corresponding predicted reward indicated as r_t^k . Upon receiving s_t^k , the prediction model generates a predicted policy p_t^k and an estimated value v_t^k . The final training loss encompasses three components: the policy loss (l_p), the value loss (l_v), and the reward loss (l_r):

$$L_{\text{MuZero}} = \sum_{k=0}^K l_p(\pi_{t+k}, p_t^k) + \sum_{k=0}^K l_v(z_{t+k}, v_t^k) + \sum_{k=1}^K l_r(u_{t+k}, r_t^k) \quad (41)$$

MuZero *Reanalyze*, as introduced in [Schrittwieser et al. \(2021\)](#), is an advanced iteration of the original MuZero algorithm. This variant enhances the model’s accuracy by conducting a fresh Monte Carlo Tree Search on sampled states with the most recent version of the model, subsequently utilizing the refined policy from this search to update the policy targets. Such reanalysis yields targets of superior quality compared to those obtained during the initial data collection phase. The [Schrittwieser et al. \(2021\)](#) expands upon this approach, formalizing it as a standalone method for policy refinement. This innovation opens avenues for its application in offline settings, where interactions with the environment are not possible.

C IMPLEMENTATION DETAILS

C.1 ENVIRONMENTS

In this section, we first introduce various types of reinforcement learning environments evaluated in the main paper and their respective characteristics, including different observation/action/reward space and transition functions.

Atari: This category includes sub-environments like *Pong*, *Qbert*, *Ms.Pacman*, *Breakout*, *UpN-Down*, and *Seaquest*. In these environments, agents control game characters and perform tasks based on pixel input, such as hitting bricks in *Breakout*. With their high-dimensional visual input and discrete action space features, Atari environments are widely used to evaluate the capability of reinforcement learning algorithms in handling visual inputs and discrete control problems.

DMControl: This continuous control suite comprises 39 continuous control tasks. Our focus here is to validate the effectiveness of ReZero in the continuous action space. Consequently, we have utilized two representative tasks (*ball_in_cup-catch* and *walker-stand*) for illustrative purposes. A comprehensive benchmark for this domain will be included in future versions.

Board Games: This types of environment includes *Connect4*, *Gomoku*, where uniquely marked boards and explicitly defined rules for placement, movement, positioning, and attacking are employed to achieve the game’s ultimate objective. These environments feature a variable discrete action space, allowing only one player’s piece per board position. In practice, algorithms utilize action mask to indicate reasonable actions.

C.2 ALGORITHM IMPLEMENTATION DETAILS

Our algorithm’s implementation is based on the open-source code of LightZero ([Niu et al., 2023](#)). Given that our proposed theoretical improvements are applicable to any MCTS-based RL method, we have chosen MuZero and EfficientZero as case studies to investigate the practical improvements in time efficiency achieved by integrating the ReZero boosting techniques: *just-in-time reanalyze* and *speedy reanalyze (temporal information reuse)*.

To ensure an equitable comparison of wall-clock time, all experimental trials were executed on a fixed single worker hardware setting consisting of a single NVIDIA A100 GPU with 30 CPU cores and 120 GiB memory. Besides, we emphasize that to ensure a fair comparison of time efficiency and sample efficiency, the model architecture and hyper-parameters used in the experiments of Section 5 are essentially consistent with the settings in LightZero. For specific hyper-parameters of *ReZero-M* and *MuZero* on Atari, please refer to the Table 3. The main different hyper-parameters in the *DMControl* task are set out in Tables 4. The main different hyper-parameters for the *ReZero-M* algorithm in the *Connect4* and *Gomoku* environment are set out in Tables 5. In addition to employing an LSTM network with a hidden state dimension of 512 to predict the value prefix ([Ye et al., 2021](#)), all hyperparameters of ReZero-E are essentially identical to those of ReZero-M in Table 3.

Wall-time statistics Note that all our current tests are conducted in the single-worker case. Therefore, the wall-time reported in Table 1 and Table 7 for reaching 100k env steps includes:

- *collect time:* The total time spent by an agent interacting with the environment to gather experience data. [Weng et al. \(2022\)](#) can be integrated to speed up. Besides, this design also makes MCTS-based algorithms compatible to existing RL exploration methods like [Burda et al. \(2018\)](#).

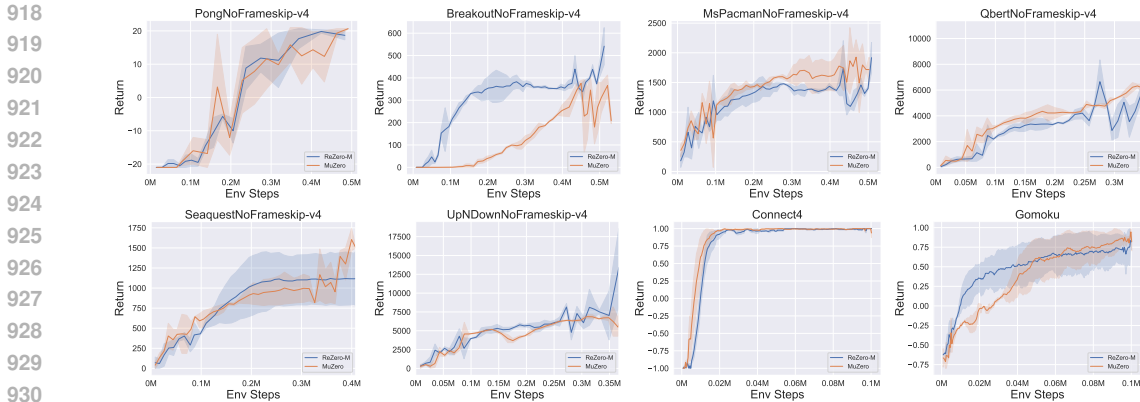


Figure 7: **Sample-efficiency** of ReZero-M vs. MuZero on six representative Atari games and two board games. The horizontal axis represents *Env Steps*, while the vertical axis indicates the *Episode Return* over 5 assessed episodes. ReZero achieves *similar* sample-efficiency than the baseline method. Mean of 5 runs; shaded areas are 95% confidence intervals.

- *reanalyze time*: The time used to reanalyze collected data with the current policy or value function for more accurate learning targets (Schrittwieser et al., 2021).
- *train time*: The duration for performing updates to the agent’s policy, value functions and model based on collected data.
- *evaluation time*: The period during which the agent’s policy is tested against the environment, separate from training, to assess performance.

Currently, we have set *collect_max_episode_steps* to 10,000 and *eval_max_episode_steps* to 20,000 to mitigate the impact of anomalously long evaluation episodes on time. In the future, we will consider conducting offline evaluations to avoid the influence of evaluation time on our measurement of time efficiency. Furthermore, the ReZero methodology represents a pure algorithmic enhancement, eliminating the need for supplementary computational resources or additional overhead. This approach is versatile, enabling seamless integration with single-worker serial execution environments as well as multi-worker asynchronous frameworks. The exploration of ReZero’s extensions and its evaluations in a multi-worker (Mei et al., 2023) paradigm are earmarked for future investigation.

Board games settings Given that our primary objective is to test the proposed techniques for improvements in time efficiency, we consider a simplified version of single-player mode in all the board games. This involves setting up a fixed but powerful expert bot and treating this opponent as an integral part of the environment. Exploration of our proposed techniques in the context of learning through self-play training pipeline is reserved for our future work.

D ADDITIONAL EXPERIMENTS

D.1 REZERO-M

In this section, we provide additional experimental results for ReZero-M. As a supplement to Table 1, Table 6 presents the complete experimental results on the 26 Atari environments. Figure 7 displays the performance over environment interaction steps of the ReZero-M algorithm compared with the original MuZero algorithm across six representative Atari environments and two board games. We can find that ReZero-M obtained *similar* sample efficiency than MuZero on the most tasks.

D.2 REZERO-E

The enhancements of ReZero we have proposed are universally applicable to any MCTS-based reinforcement learning approach theoretically. In this section, we integrate ReZero with EfficientZero to obtain the enhanced ReZero-E algorithm. We present the empirical results comparing ReZero-E with the standard EfficientZero across four Atari environments.

Hyperparameter	Value
Replay Ratio (Schwarzer et al., 2023)	0.25
Reanalyze frequency	1
Num of frames stacked	4
Num of frames skip	4
Reward clipping (Mnih et al., 2013)	True
Optimizer type	Adam
Learning rate	3×10^{-3}
Discount factor	0.997
Weight of policy loss	1
Weight of value loss	0.25
Weight of reward loss	1
Weight of policy entropy loss	0
Weight of SSL (self-supervised learning) loss (Ye et al., 2021)	2
Batch size	256
Model update ratio	0.25
Frequency of target network update	100
Weight decay	10^{-4}
Max gradient norm	10
Length of game segment	400
Replay buffer size (in transitions)	1e6
TD steps	5
Number of unroll steps	5
Use augmentation	True
Discrete action encoding type	One Hot
Normalization type	Layer Normalization
Priority exponent coefficient (Schaul et al., 2015)	0.6
Priority correction coefficient	0.4
Dirichlet noise alpha	0.3
Dirichlet noise weight	0.25
Number of simulations in MCTS (sim)	50
Categorical distribution in value and reward modeling	True
The scale of supports used in categorical distribution (Pohlen et al., 2018)	300

Table 3: Key hyperparameters of **ReZero-M** on *Atari* environments.

Hyperparameter	Value
Replay ratio (Schwarzer et al., 2023)	0.25
Reanalyze frequency	1
Batch size	64
Num of frames stacked	1
Num of frames skip	2
Discount factor	0.997
Length of game segment	8
Use augmentation	False
Number of simulations in MCTS (sim)	50
Number of sampled actions (Hubert et al., 2021)	20

Table 4: Key hyperparameters of **ReZero-M** on two *DMControl* tasks (*ball.in.cup.catch* and *walker-stand*). More experiments about this hyper-parameter will be explored in the future version. Other unmentioned parameters are the same as that in *Atari* settings.

Figure 8 shows that ReZero-E is better than EfficientZero in terms of time efficiency. Figure 9 indicates that ReZero-E matches EfficientZero’s sample efficiency across most tasks. Additionally, Table 7 details training times to 100k environment steps, revealing that ReZero-E is significantly faster than baseline methods on most games.

1026
1027
1028
1029
1030
1031
1032
1033
1034
1035
1036
1037
1038

Hyperparameter	Value
Replay ratio (Schwarzer et al., 2023)	0.25
Reanalyze frequency	1
Board size	6x7; 6x6
Num of frames stacked	1
Discount factor	1
Weight of SSL (self-supervised learning) loss	0
Length of game segment	18
TD steps	21; 18
Use augmentation	False
Number of simulations in MCTS (sim)	50
The scale of supports used in categorical distribution	10

Table 5: Key hyperparameters of **ReZero-M** on *Connect4* and *Gomoku* environments. If the parameter settings of these two environments are different, they are separated by a semicolon.

1041
1042
1043
1044
1045
1046
1047
1048
1049
1050
1051
1052
1053
1054
1055
1056
1057
1058
1059
1060
1061
1062
1063
1064
1065
1066
1067

Env. Name	ReZero-M	MuZero
Alien	1.6±0.2	8.6±0.4
Amidar	1.5±0.2	8.1±0.3
Assault	1.5±0.1	7.5±0.1
Asterix	1.3±0.1	7.2±0.2
BankHeist	2.9±0.3	8.9±0.6
BattleZone	2.2±0.3	9.6±0.6
ChopperCommand	3.4±0.4	9.0±0.7
CrazyClimber	2.7±0.1	9.1±0.4
DemonAttack	1.1±0.1	6.8±0.8
Freeway	1.0±0.0	6.1±0.2
Frostbite	2.2±0.4	10.9±0.8
Gopher	3.2±0.6	8.1±0.8
Hero	2.5±0.4	9.9±0.6
Jamesbond	2.2±0.3	9.1±0.5
Kangaroo	2.0±0.2	8.6±0.8
Krull	1.8±0.1	7.7±0.3
KungFuMaster	1.3±0.1	7.6±0.7
PrivateEye	1.0±0.1	5.8±0.5
RoadRunner	1.5±0.2	9.0±0.3
UpNDown	1.4±0.1	7.2±0.4
Pong	1.0±0.1	4.0±0.5
MsPacman	1.4±0.2	6.9±0.3
Qbert	1.3±0.1	7.0±0.3
Seaquest	1.9±0.4	10.1±0.5
Boxing	1.1±0.0	6.6±0.1
Breakout	3.0±0.8	4.9±1.8

Table 6: **Average wall-time**(hours) of ReZero-M vs. MuZero on 26 Atari game environments. The time represents the average total wall-clock time to 100k environment steps. Mean and standard deviation over 5 runs.

1071
1072
1073
1074

D.3 MORE ABLATIONS

1075
1076
1077
1078
1079

This section presents the results of three supplementary ablation experiments. Figure 10 illustrates the impact of using backward-view reanalyze within the ReZero framework on sample efficiency. The results indicate that backward-view reanalyze, by introducing root value as auxiliary information, achieves higher sample efficiency, aligning with the theoretical analysis regarding regret upper bound. Figure 11 demonstrates the effects of different action selection methods during the collect phase. The findings reveal that sampling actions directly from the distribution output by the policy

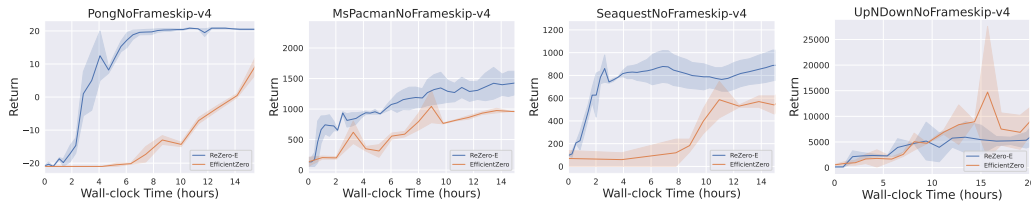


Figure 8: **Time-efficiency** of ReZero-E vs. EfficientZero on four representative Atari games. The horizontal axis represents *Wall-time* (hours), while the vertical axis indicates the *Episode Return* over 5 assessed episodes. ReZero-E achieves higher time-efficiency than the baseline method. Mean of 5 runs; shaded areas are 95% confidence intervals.

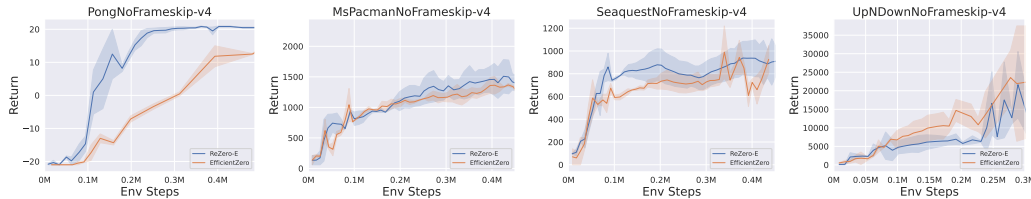


Figure 9: **Sample-efficiency** of ReZero-E vs. EfficientZero on four representative Atari games. The horizontal axis represents *Env Steps*, while the vertical axis indicates the *Episode Return* over 5 assessed episodes. ReZero-E achieves similar sample-efficiency than the baseline method. Mean of 5 runs; shaded areas are 95% confidence intervals.

<i>avg. wall time (h) to 100k env. steps</i> ↓	Pong	MsPacman	Seaquest	UpNDown
ReZero-E (ours)	2.3±1.4	3±0.3	3.1±0.1	3.6±0.2
EfficientZero (Ye et al., 2021)	10±0.2	12±1.3	15±2.3	15±0.7

Table 7: **Average wall-time** of ReZero-E vs. EfficientZero on four Atari games. The time represents the average total wall-time to 100k environment steps for each algorithm. Mean and standard deviation over 5 runs.

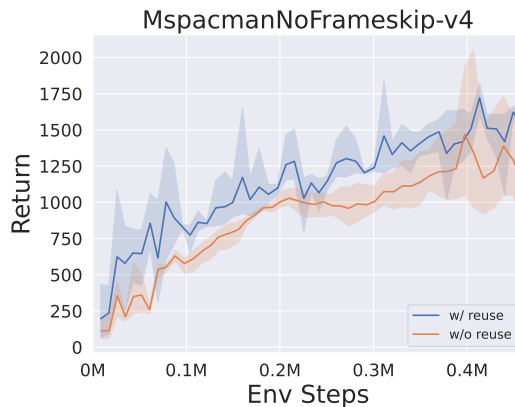


Figure 10: The results of the ablation study comparing the use of backward-view reanalyze versus its absence. Mean of 3 runs; shaded areas are 95% confidence intervals.

network does not significantly degrade the experimental results compared to using MCTS for action selection. Figure 12 depicts the relationship between the average MCTS search duration and the batch size. We set a baseline batch size of 256 and experimented with search sizes ranging from 1 to 20 times the baseline, calculating the average time required to search 256 samples by dividing the total search time by the multiplier. The results suggest that larger batch sizes can better leverage the advantages of parallelized model inference and data processing. However, when the batch size becomes excessively large, constrained by the limits of hardware resources (memory, CPU), the search

1134
 1135
 1136
 1137
 1138
 1139
 1140
 1141
 1142
 1143
 1144
 1145
 1146
 1147
 1148
 1149
 1150
 1151
 1152
 1153
 1154
 1155
 1156
 1157
 1158
 1159
 1160
 1161
 1162
 1163
 1164
 1165
 1166
 1167
 1168
 1169
 1170
 1171
 1172
 1173
 1174
 1175
 1176
 1177
 1178
 1179
 1180
 1181
 1182
 1183
 1184
 1185
 1186
 1187

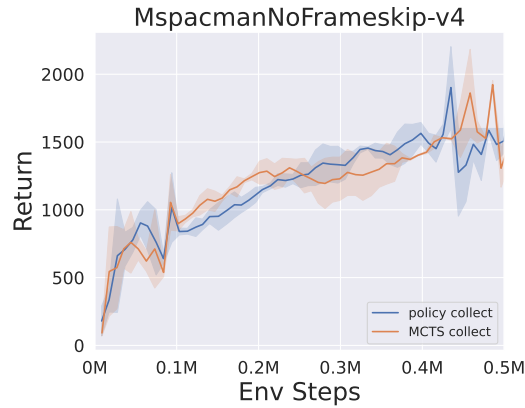


Figure 11: The comparison of the outcomes of sampling actions based on the policy network’s output against selecting actions using MCTS. Mean of 3 runs; shaded areas are 95% confidence intervals.

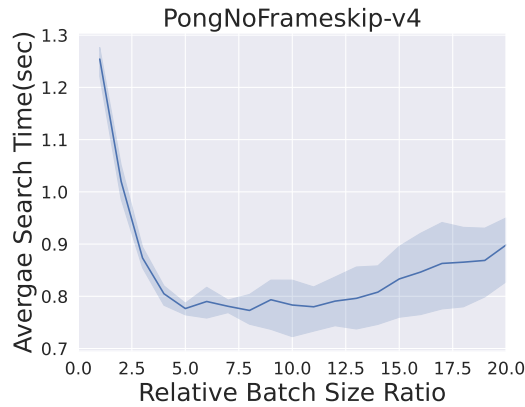


Figure 12: The depiction of the variation in the average search speed of MCTS as the batch size increases. Mean of 3 runs; shaded areas are 95% confidence intervals.

speed cannot increase further and may even slightly decrease. We ultimately set the batch size to 2000, which yields the fastest average search speed on our device.

1188 D.4 TOY CASE
1189

1190 We offer the complete code for the toy case. Readers can compare the core functions *search()* and
1191 *reuse_search()* of the MCTS class to understand how root node values are utilized and compare
1192 *select()* and *reuse_select()* to understand how the search process is prematurely halted.

```

1193 import random
1194 import math
1195 import time
1196 import numpy as np
1197 import matplotlib.pyplot as plt
1198
1199 class Node:
1200     def __init__(self, state, parent=None):
1201         self.state = state
1202         self.parent = parent
1203         self.children = []
1204         self.visits = 0
1205         self.value = 0
1206
1207     def is_fully_expanded(self):
1208         return len(self.children) == len(self.state.get_possible_actions())
1209
1210     def add_child(self, child_state):
1211         child = Node(child_state, self)
1212         self.children.append(child)
1213         return child
1214
1215 class MCTS:
1216     def __init__(self, exploration_weight=1.0):
1217         self.exploration_weight = exploration_weight
1218         self.gamma = 0.9
1219
1220     # the search process in origin MCTS
1221     def search(self, initial_state, max_iter=100):
1222         root = Node(initial_state)
1223
1224         for _ in range(max_iter):
1225             node = self.select(root)
1226             reward = self.simulate(node.state)
1227             self.backpropagate(node, reward)
1228
1229             best_child = self.get_best_child(root, 0)
1230             return best_child.state.current_pos, root.value
1231
1232     # the search process in our accelerated MCTS by reuse the root value
1233     def reuse_search(self, initial_state, value, action, max_iter=100):
1234         root = Node(initial_state)
1235
1236         for _ in range(max_iter):
1237             node = self.reuse_select(root, action)
1238             if node.state.current_pos == action:
1239                 reward = value
1240             else:
1241                 reward = self.simulate(node.state)
1242             self.backpropagate(node, reward)
1243             best_child = self.get_best_child(root, 0)
1244             return best_child.state.current_pos, root.value
1245
1246     # select nodes in origin MCTS
1247     def select(self, node):
1248         while not node.state.is_terminal():
1249             if not node.is_fully_expanded():
1250                 return self.expand(node)
1251             else:
1252                 node = self.get_best_child(node, self.exploration_weight)
1253         return node
1254
1255     # select nodes in our accelerated MCTS by reuse the root value
1256     def reuse_select(self, node, actionpos):
1257         while not (node.state.is_terminal() or node.state.current_pos == actionpos):
1258             if not node.is_fully_expanded():
1259                 return self.expand(node)
1260             else:
1261                 node = self.get_best_child(node, self.exploration_weight)
1262         return node
1263
1264     def expand(self, node):
1265         actions = node.state.get_possible_actions()
1266         for action in actions:
1267             if not any(child.state.current_pos == node.state.copy().step(action)[0] for child in node.children):
1268                 new_state = node.state.copy()
1269                 new_state.step(action)
1270                 return node.add_child(new_state)
1271         return None
1272
1273     def simulate(self, state):
1274         sim_state = state.copy()

```

```

1242     count = 1
1243     while not sim_state.is_terminal():
1244         action = random.choice(sim_state.get_possible_actions())
1245         sim_state.step(action)
1246         count += 1
1247     return sim_state.get_reward()/count
1248
1249 def backpropagate(self, node, reward):
1250     gamma = self.gamma
1251     while node is not None:
1252         node.visits += 1
1253         node.value += reward * gamma
1254         node = node.parent
1255         gamma *= self.gamma
1256
1257 def get_best_child(self, node, exploration_weight):
1258     best_value = -float('inf')
1259     best_children = []
1260     for child in node.children:
1261         exploit = child.value / child.visits
1262         explore = math.sqrt(2.0 * math.log(node.visits) / child.visits)
1263         value = exploit + exploration_weight * explore
1264         if value > best_value:
1265             best_value = value
1266             best_children = [child]
1267         elif value == best_value:
1268             best_children.append(child)
1269     return random.choice(best_children)
1270
1271 class GridWorld:
1272     def __init__(self):
1273         self.grid = [[0 for _ in range(4)] for _ in range(4)]
1274         self.start_pos = (0, 0)
1275         self.goal_pos = (0, 3)
1276         self.current_pos = self.start_pos
1277         self.actions = ['down', 'up', 'left', 'right']
1278
1279     def reset(self):
1280         self.current_pos = self.start_pos
1281         return self.current_pos
1282
1283     def step(self, action):
1284         if action not in self.actions:
1285             raise ValueError("Invalid_action")
1286
1287         x, y = self.current_pos
1288
1289         if action == 'up':
1290             x = max(0, x - 1)
1291         elif action == 'down':
1292             x = min(3, x + 1)
1293         elif action == 'left':
1294             y = max(0, y - 1)
1295         elif action == 'right':
1296             y = min(3, y + 1)
1297
1298         self.current_pos = (x, y)
1299         reward = 1 if self.current_pos == self.goal_pos else 0
1300         done = self.current_pos == self.goal_pos
1301
1302         return self.current_pos, reward, done
1303
1304     def is_terminal(self):
1305         return self.current_pos == self.goal_pos
1306
1307     def get_reward(self):
1308         return 1 if self.current_pos == self.goal_pos else 0
1309
1310     def get_possible_actions(self):
1311         x, y = self.current_pos
1312         possible_actions = []
1313
1314         if x > 0:
1315             possible_actions.append('up')
1316         if x < 3:
1317             possible_actions.append('down')
1318         if y > 0:
1319             possible_actions.append('left')
1320         if y < 3:
1321             possible_actions.append('right')
1322
1323         return possible_actions
1324
1325     def copy(self):
1326         new_grid = GridWorld()
1327         new_grid.current_pos = self.current_pos
1328         return new_grid
1329
1330     def render(self):

```



```

1296     for i in range(4):
1297         for j in range(4):
1298             if (i, j) == self.current_pos:
1299                 print("A", end=" ")
1300             elif (i, j) == self.goal_pos:
1301                 print("G", end=" ")
1302             else:
1303                 print(".", end=" ")
1304             print()
1305         print()
1306
1307 class GridWorldWithWalls:
1308     def __init__(self):
1309         self.grid = [[0 for _ in range(7)] for _ in range(7)]
1310         self.start_pos = (0, 0)
1311         self.goal_pos = (6, 6)
1312         self.current_pos = self.start_pos
1313         self.actions = ['down', 'up', 'left', 'right']
1314         self.walls = [(2, 2), (2, 3), (1,1), (3, 2), (3, 4), (3,2), (0,5), (4, 4), (6,3), (5,3)]
1315
1316         for wall in self.walls:
1317             self.grid[wall[0]][wall[1]] = 1
1318
1319     def reset(self):
1320         self.current_pos = self.start_pos
1321         return self.current_pos
1322
1323     def step(self, action):
1324         if action not in self.actions:
1325             raise ValueError("Invalid action")
1326
1327         x, y = self.current_pos
1328
1329         if action == 'up':
1330             x = max(0, x - 1)
1331         elif action == 'down':
1332             x = min(6, x + 1)
1333         elif action == 'left':
1334             y = max(0, y - 1)
1335         elif action == 'right':
1336             y = min(6, y + 1)
1337
1338         if (x, y) not in self.walls:
1339             self.current_pos = (x, y)
1340
1341         reward = 1 if self.current_pos == self.goal_pos else 0
1342         done = self.current_pos == self.goal_pos
1343
1344         return self.current_pos, reward, done
1345
1346     def is_terminal(self):
1347         return self.current_pos == self.goal_pos
1348
1349     def get_reward(self):
1350         return 1 if self.current_pos == self.goal_pos else 0
1351
1352     def get_possible_actions(self):
1353         x, y = self.current_pos
1354         possible_actions = []
1355
1356         if x > 0 and (x - 1, y) not in self.walls:
1357             possible_actions.append('up')
1358         if x < 6 and (x + 1, y) not in self.walls:
1359             possible_actions.append('down')
1360         if y > 0 and (x, y - 1) not in self.walls:
1361             possible_actions.append('left')
1362         if y < 6 and (x, y + 1) not in self.walls:
1363             possible_actions.append('right')
1364
1365         return possible_actions
1366
1367     def copy(self):
1368         new_grid = GridWorldWithWalls()
1369         new_grid.current_pos = self.current_pos
1370         return new_grid
1371
1372     def render(self):
1373         for i in range(7):
1374             for j in range(7):
1375                 if (i, j) == self.current_pos:
1376                     print("A", end=" ")
1377                 elif (i, j) == self.goal_pos:
1378                     print("G", end=" ")
1379                 elif (i, j) in self.walls:
1380                     print("#", end=" ")
1381                 else:
1382                     print(".", end=" ")
1383             print()
1384         print()

```

```

1350
1351
1352 env = GridWorldWithWalls()
1353 mcts = MCTS()
1354
1355 # plot the grid
1356 plt.figure(figsize=(6, 6))
1357 plt.matshow(env.grid, cmap='binary', fignum=0, vmin=0, vmax=1)
1358
1359 for i in range(7):
1360     for j in range(7):
1361         if (i, j) == env.start_pos:
1362             plt.text(j, i, 'A', ha='center', va='center', color='black', fontsize=12)
1363         elif (i, j) == env.goal_pos:
1364             plt.text(j, i, 'G', ha='center', va='center', color='black', fontsize=12)
1365         elif (i, j) in env.walls:
1366             plt.text(j, i, '|', ha='center', va='center', color='black', fontsize=12)
1367         else:
1368             plt.text(j, i, ' ', ha='center', va='center', color='black', fontsize=12)
1369
1370 for wall in env.walls:
1371     plt.gca().add_patch(plt.Rectangle((wall[1] - 0.5, wall[0] - 0.5), 1, 1, color='black'))
1372
1373 for i in range(7):
1374     for j in range(7):
1375         plt.gca().add_patch(plt.Rectangle((j - 0.5, i - 0.5), 1, 1, fill=False, edgecolor='black', linewidth=2))
1376
1377 plt.title('GridWorld_Environment', fontsize=24)
1378 plt.xticks(np.arange(7), ['0', '1', '2', '3', '4', '5', '6'])
1379 plt.yticks(np.arange(7), ['0', '1', '2', '3', '4', '5', '6'])
1380 plt.xlabel('Column', fontsize=24)
1381 plt.ylabel('Row', fontsize=24)
1382 plt.show()
1383
1384 # record the search time
1385 search_times = np.zeros((7, 7))
1386 reuse_times = np.zeros((7, 7))
1387 for i in range(7):
1388     for j in range(7):
1389         if (i, j) == env.goal_pos or (i, j) in env.walls:
1390             continue
1391
1392         env.current_pos = (i, j)
1393         print(f"Starting_MCTS_from_position:_{env.current_pos}")
1394
1395         start_time = time.time()
1396         reuse_action, root_value = mcts.search(env)
1397         end_time = time.time()
1398         search_time = end_time - start_time
1399         search_times[i, j] = search_time
1400
1401         env.current_pos = reuse_action
1402         if reuse_action == env.goal_pos:
1403             reuse_value = 1
1404         else: _, reuse_value = mcts.search(env)
1405
1406         env.current_pos = (i, j)
1407         start_time = time.time()
1408         best_action, root_value = mcts.reuse_search(env, reuse_value, reuse_action)
1409         end_time = time.time()
1410         reuse_time = end_time - start_time
1411         reuse_times[i, j] = reuse_time
1412
1413         print(f"Best_action_leads_to_position:_{reuse_action}")
1414         print(f"Reuse_search_best_action_leads_to_position:_{best_action}")
1415         print(f"Search_time:_{search_time:.4f}_seconds")
1416         print(f"reuseSearch_time:_{reuse_time:.4f}_seconds\n")
1417
1418 # plot the time heatmap
1419 plt.figure(figsize=(6, 6))
1420 plt.imshow(search_times, cmap='viridis', vmin=0, vmax=0.2, interpolation='nearest')
1421 plt.colorbar(label='Search_Time_(seconds)')
1422 plt.title('Origin_Search_Time', fontsize=20)
1423 plt.xticks(np.arange(7), ['0', '1', '2', '3', '4', '5', '6'])
1424 plt.yticks(np.arange(7), ['0', '1', '2', '3', '4', '5', '6'])
1425 plt.xlabel('Column', fontsize=20)
1426 plt.ylabel('Row', fontsize=20)
1427 plt.figure(figsize=(6, 6))
1428 plt.imshow(reuse_times, cmap='viridis', vmin=0, vmax=0.2, interpolation='nearest')
1429 plt.colorbar(label='Search_Time_(seconds)')
1430 plt.title('Accelerated_Search_Time', fontsize=20)
1431 plt.xticks(np.arange(7), ['0', '1', '2', '3', '4', '5', '6'])
1432 plt.yticks(np.arange(7), ['0', '1', '2', '3', '4', '5', '6'])
1433 plt.xlabel('Column', fontsize=20)
1434 plt.ylabel('Row', fontsize=20)
1435 plt.show()

```